Hot-cool box calorimetric determination of the solar heat gain coefficient and the *U*-value of internal shading devices

Ayelén Villalba, [1]✉

Phone +54 261 5244310
Email avillalba@mendoza-conicet.gob.ar

Erica Correa, [1]

Andrea Pattini, [1]

Daniel Vicare, [2]

[1] INAHE (Institute of Environment, Habitat and Energy), CCT–Mendoza (Scientific and Technological Centre Mendoza), CONICET (National Scientific and Technical Research Council), CC 131 5500 Mendoza, Argentina AQ1

[2] CCT–Mendoza (Scientific and Technological Centre Mendoza)–CONICET, (National Scientific and Technical Research Council), CC 131 5500 Mendoza, Argentina

Abstract

In several developing countries, energy performance rating programs are currently in progress. Complex fenestration systems (CFS) are building components that play a key role in reducing energy consumption. The development and testing of equipment is central for beginning the energy efficiency rating process of complex glazing systems in these countries. This paper validates the use of a low-cost hot-cold box calorimeter for measurement of the solar heat gain coefficient (SGHC) and overall heat transfer coefficient (*U*-value) of interior shading systems. This work aims to determine the energy performance of three types of often employed shading systems: solar control films, interior horizontal venetian blinds, and indoor drapery curtains. Results show that the energy performance of solar shading devices studied depends on both their morphological and optical properties. The shading systems analyzed present similar *U*-values, where technological features are represented by the thickness and the thermal conductivity of the material. SHGC is mainly defined by the transmittance and, to a lesser extent,

the absorptance of the systems, which differ significantly according to the analyzed shading device. The three types of curtains analyzed demonstrate an SHGC dependent on the fabrics openness factor: jacquard curtains (openness factor 0.05) present a SHGC of 0.7, whereas organza curtains (openness factor 0.45) have a SHGC of 0.82. The SHGC of the venetian blinds analyzed varies on average 36% according to the slat tilt (0°–45°). The solar control films examined modify their solar gain according to their spectral selectivity.

Keywords

Solar control systems
Hot-cool box calorimeter
Solar heat gain coefficient
U-value

Introduction

AQ2

The building envelope plays a key role in building energy consumption—heating and cooling—and in visual and thermal comfort because it is the primary barrier between the interior and the exterior (IEA 2013). In developing countries with warm climates, energy consumption for cooling will increase between 300 and 600%. In warm climates, low-cost solutions such as reflective walls and roofs, exterior shading systems, and energy-efficient windows can help reduce this consumption. On the other hand, in cold climates, complex window systems can be used for passive heating, reducing energy consumption (IEA 2013). The successful implementation of complex glazing systems can achieve savings for lighting, up to 60%, and for refrigeration, up to 20% (IEA 2013).

Shading systems can significantly decrease energy consumption as well as improve thermal comfort and reduce potential glare problems (Wall and Bülow-Hübe 2003). Window attachments have the economic potential to save nearly 844 ZJ in cooling and heating energy by 2030 (Curcija 2016). Recent studies (Lau et al. 2016) carried out for high-rise office buildings in hot climates show that the use of various shading devices on low-e double-glazed facades will result between 1.0 and 3.4% annual cooling energy savings, depending on the types of shading devices and facade orientations. The estimated annual cooling energy savings increase to between 5.0 and 9.9% when the shading devices are applied to all orientations of low-e double-glazed facades. Studies that focus on internal dynamic solar shading show that significant cooling energy savings can be achieved, despite their high solar transmittance when compared to external solar shading. The use of internal shading devices has shown energy savings for

cooling from 24 to 36%, depending on climate conditions and type of glazing used (Hutchins 2015). This is important since internal shading can also provide significant heating energy savings and increase thermal and visual comfort for the building user (Hutchins 2015).

This is why worldwide window certification is currently focused on analyzing the energy performance of solar control elements which are part of CFS (Selkowitz 2011). Energy rates that qualify the energy performance of shading device are the same as those used for windows: overall heat transfer coefficient (*U*-value), solar heat gain coefficient (SHGC), and visible transmittance (VT). Many associations have been set up with the aim of analyzing the energy performance of shading systems: AURINKO (Finland), ASSITES (Italy), ITRS (Germany), USR (Switzerland), NFRC (USA), AERC (USA), Romazo (Netherlands), FFB (France), BBSA (England), and Verozo (Belgium), among others.

On a local scale, rising energy prices and the progressive withdrawal of energy subsidies have led to focus on building energy efficiency. In Argentina, there are programs focused on reducing the growing energy consumption of commercial and public buildings. The most relevant of these programs is PRONUREE (National Program for the Rational and Efficient Energy Use) (PRONUREE 2015) supported by the National Department of Energy. This program has implemented an energy efficiency labeling system to identify the energy consumption of machines, appliances, and artificial lights. However, at present, certification does not apply to building components. Although in Argentina window energy performance labels do not yet exist, the subcommittee of the IRAM standard 11507 is considering the energy characterization of windows through rates that take into account energy exchanges—conduction, convection, and radiation (gains and loss).

Within this context, this work aims to determine the energy performance rates (*U* and SHGC) of three types of often employed shading systems—solar control films, interior horizontal venetian blinds, and indoor drapery curtains—using a low-cost hot-cool box calorimetric steady-state test facility. The measured values of *U* and SHGC are compared to literature values, and a comparative analysis is done in order to assess the differences between the studied shading devices. This paper focuses on the analysis of the energy performances of locally used shading devices. The aim of this investigation is to develop local capacities for the assessment of CFS energy efficiency rates concerning experimental and simulation methods. Furthermore, the goal is to collaborate in the energy certification process of building components—shading devices—that the country is currently undergoing.

Theoretical background

Test facilities for measurement of SHGC and *U*-value

Testing equipment has been developed in different places around the world aiming to assess the energy performance of windows and shading systems. Some measurements are made indoors under controlled conditions and others are outdoors (Dubois 1997; Álvarez et al. 2000; Chen and Wittkopf 2012; Harrison and Collins 1999; Inoue and Momota 2006; Klems et al. 1982; Kuhn 2014; Marinoski et al. 2012; Wall and Bülow-Hübe 2003). Three types of outdoor calorimeters can be identified. Harrison and Collins (1999) developed a solar calorimeter capable of following the solar path through a solar tracker. Klems et al. (1982), Wall and Bülow-Hübe (2003), and Marinoski et al. (2012) built mobile solar calorimeters for field measurement using a double hot box arrangement. In 2006, Inoue and Momota developed an on-site method for evaluating the solar shading performance of advanced windows. This is particularly interesting for very windy conditions in the top stories of high-rise buildings. With respect to indoor test facilities, in 2000, Álvarez et al. built a calorimeter test box and solar simulator for different types of glazing solar gain measurement. Wall and Bülow-Hübe (2003) set up a test facility with improvements in the solar simulator (lamp cluster), controlled wind speed, and other features that enable measurements of windows with sunshade. Chen and Wittkopf (2012) present a calorimetric hot box with two main components: the metering and surrounding guarding box (indoor side) and the climate box (outdoor side). This facility was also used by Ng (2014) in his studies about semitransparent building-integrated photovoltaic (BIPV) windows. Kuhn (2014) uses a calorimetric device for the determination of solar heat gain coefficient under steady-state laboratory conditions with two different approaches of calorimetric measurement: cooled plate method and cooled box method. The National Solar Test Facility (NSTF) test facility of Canada has a solar simulator and a solar calorimeter that can make measurements under a variety of imposed weather conditions in a large environmentally controlled chamber (Kotey et al. 2009, Natural Resources Canada 2017). The current work comments only briefly on the broad amount of test facilities built around the world and the documents that are referenced can be seen for further information.

Solar shading devices: solar control films, horizontal venetian blinds, and indoor drapery curtains

Dubois (1997) provides a thorough analysis of research developed between 1963 and 1996 about solar shading devices (thermal and solar transmittance).

Álvarez et al. (2000) analyzed the changes in energy performance (*U*-value and SHGC) of glass with different surface treatments. The authors conclude that the glazing with reflective treatment (reflectasol) has the lowest shading coefficient (0.36). Chaiyapinunt et al. (2005) state that films, according to their optical properties, have a significant effect in reducing the solar gain of windows. However, they have a weak influence on gains due to thermal conduction.

Regarding the energy performance of blinds, previous studies show that in facades with adaptive dynamic properties (venetian blinds, louvers) solar heat gain coefficient varies according to the system arrangement, particularly to slats tilt angle (Kuhn 2014; Simmler and Binder 2008; Kotey et al. 2009). It has also been proven that the thermal behavior of venetian blinds varies according to other optical and geometric properties such as slat curvature, the distance between slats, and slat surface reflectance (Chaiyapinunt and Khamporn 2014; Collins and Harrison 1999; Simmler and Binder 2008; Sharda and Kumar 2016). Kotey et al. (2009) determined that for the same slat angle, the SHGC varies according to surface optical properties (white venetian blind (slat angle = 60°), SGHC = 0.46; black venetian blind (slat angle = 60°), SGHC = 0.67). Chaiyapinunt and Khamporn (2014) observed that the slat reflectance of the venetian blind has a direct effect on the shortwave SHGC and that the slat absorptance of the venetian blind has a direct effect on the longwave SHGC. They also demonstrate that slats with more curvature (lower value of slat radius of curvature) reduce more the SHGC caused by direct solar radiation when compared to slats with less curvature. Furthermore, some studies show that the energy performance of venetian blinds is influenced by external factors such as the incident radiation wavelength and source position (Chaiyapinunt and Khamporn 2014; Kuhn 2014).

Regarding the thermal transmittance of curtains, many studies prove that sealing edges of draperies around the window increase thermal performance (Grasso et al. 1990 and Lunde and Lindley 1988 as cited in Dubois 1997) and that opaque fabrics (draperies) provide better insulation (by 5%) than transparent or translucent fabrics. In 2009, Kotey et al. studied the solar heat gain and solar transmittance of roller blinds, insect screens, and pleated drapes. They measured a SHGC value of 0.43 for a beige pleated drape (closed weave, 100% fullness).

The energy ratings of complex glazing systems

U-value and SHGC of shading devices are influenced by various energy exchange phenomena. These phenomena include power flows through the window caused by heat transfer, by thermal conduction and convection due to the temperature difference between the indoor and outdoor air, longwave

radiation exchange between the window and its surroundings and between the layers of glazing, and shortwave energy flow between the window and the environment and between glazing layers (ASHRAE 2009).

Simplified calculations assume that temperatures of the sky, ground, and surrounding objects correlate with the outdoor air temperature and that all the radiating surfaces are at the same temperature as the outdoor air. The basic equation for energy flow in steady state for a fenestration system (ASHRAE 2009) (Eq. 1) is

$$q = U * A * (T_{\mathrm{o}} - T_{\mathrm{i}}) + \mathrm{SHGC} * A * E \quad (1)$$

where q: energy flow [W], U: overall heat transfer coefficient [W/m^2 K], A: projected area of the window [m^2], T_{o}: outside air temperature [K], T_{i}: inside air temperature [K], SHGC: solar heat gain coefficient, and E: total incident radiation [W/m^2].

The overall heat transfer coefficient (U-value) (Eq. 3) and the solar heat gain coefficient (SHGC) (Eq. 4) are rates that assess the energy performance of a fenestration system in a steady state. The major advantage of Eq. 1 is its simplicity, achieved by clustering together all energy transfer processes—conduction, convection, and radiation—in U and SHGC. These amounts vary due to several factors: (1) convective heat transfer rates are modified according to the interior-exterior temperature difference and wind speed, (2) window systems always involve at least two thermal resistances in series, and (3) solar heat gain coefficient varies according to solar incident angle and spectral distribution.

Energy flow is divided into two terms (Eq. 2), where Q_{t} is the steady-state heat transfer caused by indoor/outdoor temperature difference (U-value [W/m^2 K]) and Q_{s} is the steady-state heat transfer caused by incident solar radiation (SHGC (dimensionless)):

$$Q = Q_{\mathrm{t}} + Q_{\mathrm{s}} \quad (2)$$

where Q_{t}: [W] and Q_{s}: [W].

$$U = \frac{1}{\frac{1}{h_{\mathrm{o}}} + \frac{1}{h_i} + \frac{L}{k}} \quad (3)$$

where h_{o}: outdoor surface heat transfer coefficients [W/(K · m ^{2})], h_{i}: indoor surface heat transfer coefficients [W/(K · m ^{2})], L: thickness [m], and k: thermal conductivity [W/(K · m)]

$$\mathrm{SGHC}\,(\theta) = T^{\mathrm{f}}\,(\theta) + \sum_{k=1}^{L} N_{\mathrm{k}}\, A_{\mathrm{k}}^{\mathrm{f}}\,(\theta) \qquad 4$$

where SGHC: solar heat gain coefficient, A: total absorptance of glazing system, N_{k}[1]: inward-flowing fraction of the absorbed transmittance, and T: transmittance of the glazing system.

SHGC and U-value are the key rates used to characterize the energy performance of a shading device; in this work, these indicators were obtained through measurements in a hot-cool box calorimeter in a steady state. The sample (shading device + clear glass 3 mm) is located in front of the box. When the SHGC measurement is performed, a cooling system is used: cool box; when the heat transfer coefficient is measured, a heating system is used: hot box. This type of setup is particularly useful for measuring internal shading systems (Kuhn 2014). The assessment is based on an energy balance (Kuhn 2014; Álvarez et al. 2000). Finally, we can state that the values of SHGC and U measured in this work are experimental laboratory values ($\mathrm{SHGC}_{\mathrm{exp}}$ and U_{exp}), as they are performed under controlled boundary conditions (Kuhn 2014).

Case study

Selection of cases is based on studies previously developed by the authors in the metropolitan area of the city of Mendoza (Author 2012), where it was determined that solar control elements most commonly used in the study area are solar control films, interior horizontal venetian blinds, and indoor drapery curtains (Table 1). The Appendix details the features of each of the selected shading systems.

Table 1

Analyzed shading devices

Typology of solar control element	Shading device	Type
Applied films	Solar control film	fxst20, fxst35, p18ar (3M^{TM})
Flexible screens	Interior drapery curtain	Organza, jacquard, polyester gabardine
Discrete systems	Horizontal interior venetian blind (slat width 17 mm; tilt angle 0°–45°)	Diffuse silver, diffuse white

AQ3

The study carried out in the city of Mendoza is in accordance with works developed internationally, which argue that despite the large number of shading devices available, the three most common dynamic shading devices are interior venetian blinds, textile curtains, and roller shades. Further studies argue that unlike dynamic shading devices, the properties of fixed shading, such as light shelves, awnings, and eaves, are generally known (Tzempelikos 2008).

Measurements were performed with two different slopes—0° and −45°—in order to take into account the changes in thermal performance of blinds according to slat inclination.

The energy performance of the solar shading selected will be analyzed combined with a clear glass (3 mm), the most common type of glass used in Argentina (de Gastines et al. 2015).

Methodology

During the course of this investigation, a low-cost hot-cold box calorimeter was built up in the INAHE (Institute of Environment, Habitat and Energy), CCT CONICET Mendoza; overall heat transfer coefficient (U) and solar heat gain coefficient (SHGC) of shading device were measured with this equipment in experimental conditions.

Shading devices (venetian blinds and drapery curtains) are fixed with a rail in the upper inner part of the calorimeter box, so as to be parallel to the glass at a distance of 3 cm. The size of the calorimeter opening is 50 cm by 50 cm (Fig. 1).

Fig. 1

Schematics of the hot-cool box calorimeter used to measure energy rates of shading device: data acquisition system plus heating system (U-value). Dimensions are in centimeters

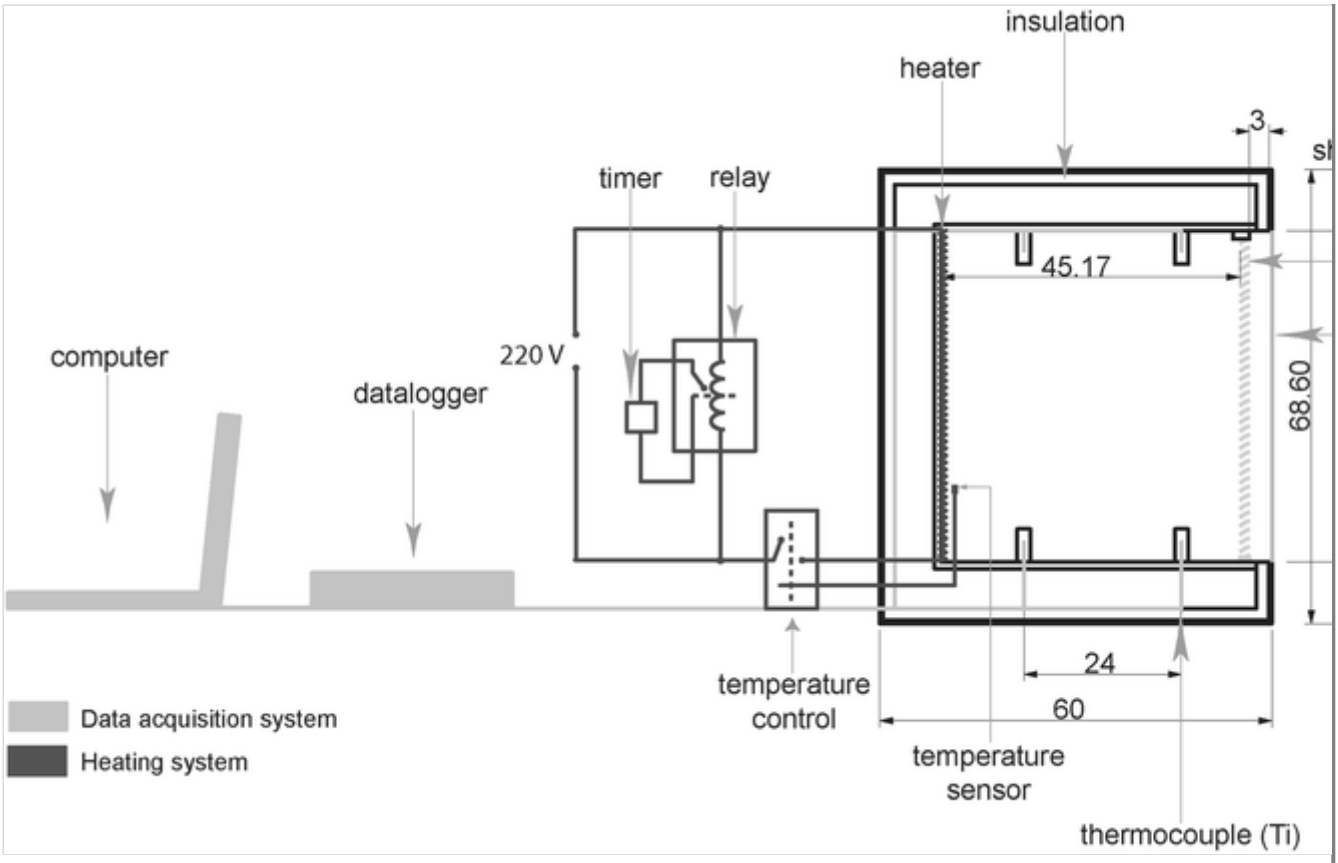

Technical description of the calorimeter

The calorimeter is based on the principle of hot-cold box. The inner walls of the box are built of polycarbonate, coated with low reflectance (0.2) black paint, insulated with 7.5 cm of expanded polystyrene. The sample holder is located on the front face of the box. On the back face of the box, the cooling or heating systems are arranged alternately, both components are removable, and the back is insulated. The entire assembly, except for the front face of the box, is covered with a reflective outer layer. The calorimeter is located in a room with an air-conditioner unit in order to keep a controlled ambient temperature.

Heating system

The electric resistance is placed on an insulating plate with the same dimensions as the inner face of the box (Fig. 1). The emitted power is 120 W. This device is regulated by a temperature control that does not allow the temperature to rise above 60 °C by activating the locking or unlocking of the circuit. This circuit is linked to a timer in order to determine the time at which the resistance operates (adding heat). In this way, one can calculate the amount of heat necessary for the system to reach thermal equilibrium with exterior conditions, once the system reaches steady state, and calculate the heat transfer coefficient.

Cooling system

The cooling system is made up of a heat exchanger placed on a copper plate (absorbing plate) in the inner rear wall of the box. This device is connected to the heat exchange fluid-water circuit, supplied by a temperature-controlled water bath (Fig. 2). Heat gains entering through the shading system are balanced with the energy extracted by the heat exchanger. Once a steady state is reached, the amount of energy entering the system through the shading device is equal to the amount of energy extracted by the water flow passing through the absorption plate. The amount of energy extracted is calculated measuring the temperature difference between inlet and outlet water flow.

Fig. 2

Schematics of the hot-cool box calorimeter used to measure energy rates of shading device: data acquisition system, solar simulator, and cooling system (SGHC). Dimensions are in centimeters

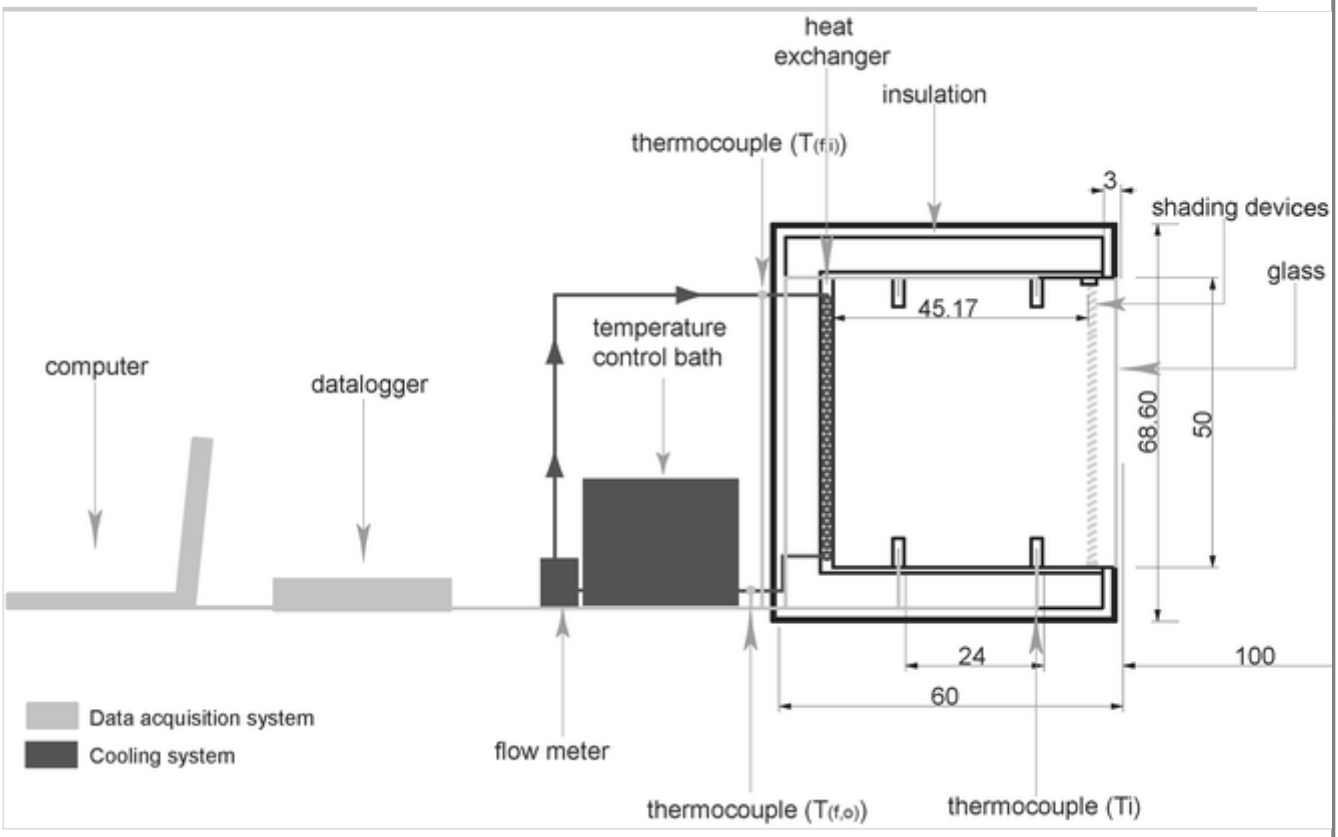

Solar simulator

The solar simulator is made up of a 1000-W/m^2 tungsten halogen lamp (Philips Halogen linear lamp 8727900881264 1000 W R7s cap 220–240 V Warm White) (Philips 2016). This lamp was selected because it provides a continuous radiative flux and its spectrum is similar to the sun's spectrum (Álvarez et al. 2000), as it displays emission spectral profiles resembling that of a blackbody radiator (Davidson 2017). The incident power was measured with a LI-200SA Pyranometer (±5%). This type of lamp was selected as it is both available in the

country where the study is performed and it is low cost, in line with the objectives of this study.

Analyzing the energy performance of facade components requires several individual measurements with different angles of incidence (Klems et al. 1982, Kuhn 2014) and with variations on incident irradiance. This is particularly important for angle-dependent sunshades, e.g., venetian blinds (Wall and Bülow-Hübe 2003). Although the test facility developed in this study does not have such capabilities, the objective of this research is to calculate energy rates for energy performance certification of local shading device. This is carried out at normal incidence on an international level (NFRC-200 2010). Consequently, as supported by the NFRC, the SHGC calculated using this procedure may not be appropriate for determining peak solar heat gains for other angles of direct beam incidence, nor for determining the solar heat gain produced by diffuse radiation incident on the fenestration system, nor for determining seasonal energy performance (NFRC-200 2010).

Irradiance uniformity Irradiance was measured with a pyranometer (Li-Cor LI-200SA) on a grid of 25 points uniformly distributed in an area of 0.5 m * 0.5 m. In order to obtain the incident radiant power (Q_{rad}), measurements are integrated over a distance of 1 m from the lamp to the front face of the box where the sample is located (Álvarez et al. 2000). A mean irradiance value of 703 W/m^2 was measured with a nonuniformity of ±10.07%.

Temporal stability In order to quantify the lamps' stability through time, incident radiation was measured with the pyranometer. The sensor was located in the center of the glazing area at a distance of 1 m from the lamp. This allowed the incident power variation in the last hour of measurement (±5.75 W/m^2) to be determined (Fig. 3).

Fig. 3

Incident radiation variability throughout the measurement

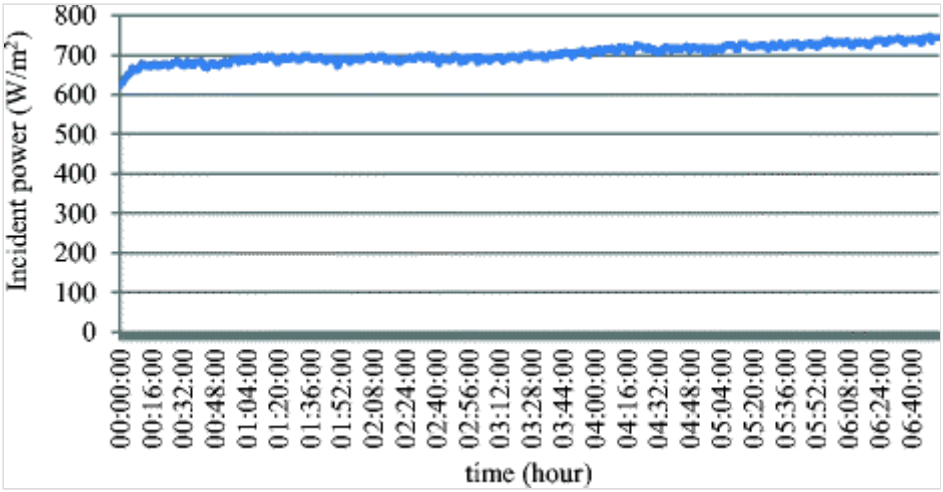

Data acquisition system

The data acquisition system consists of 16 type T thermocouples (Fig. 4, Table 2), protected from direct radiation—radiation shields—arranged as shown in Fig. 3, connected to a data logger. This measuring device is connected to a computer, which through the software MEDTEMP logs temperature data in a spreadsheet—Excel (the MEDTEMP software was adjusted for the purposes of this study by Dr. Ernesto Betman, INAHE-CCT Mendoza, within the framework of Project 0133 ENARGAS-PICTO ANPCyT).

Fig. 4

Arrangement of type T thermocouples in hot box: front view (**a**), perspective view (**b**)

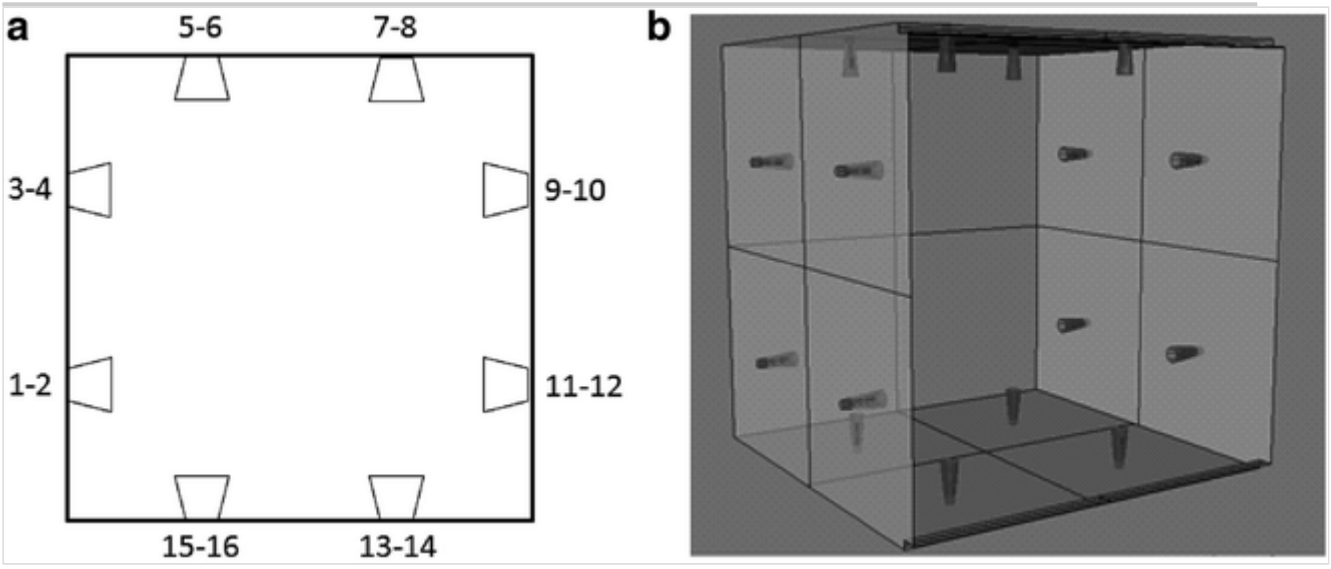

Table 2

Information about the sensors

Sensor	Absolute value of reference	Uncertainty

Sensor	Absolute value of reference	Uncertainty (%)	Uncertainty (Absolute)
Thermocouple (°C)	0.5	8.00	0.04
Pyranometer (W/m^2)	703	10.07	71.55
Flow meter (L/s)	0.076	10.68	0.01

(%) (Absolute)

The system is completed with a data logger for type T thermocouples (Table 2), that logs the temperature of the fluid entering and exiting the heat exchanger and the ambient temperature of the room where the test is performed.

Measurement and calculation of *U*-value

For this procedure, the heating system was used, and inside and outside temperatures were recorded until a steady state was reached. The overall heat transfer coefficient, U_{exp}, was determined by the average of the indoor and outdoor temperatures, measured at steady state, and the power supplied by the electrical resistance (heater) (Eq. 5):

$$U_{\text{exp}} = \frac{Q_{\text{heater}}}{A\,(T_{\text{i}} - T_{\text{o}})} \quad 5$$

where A, the area of the box [m^2]; T_{i}, the indoor mean temperature in steady state [K]; $T_{\text{o,}}$ the outdoor mean temperature in steady state [K]; and Q_{heater}, the power provided by the electrical resistance [W].

Heat loss is calculated from the energy balance; in steady state $Q_{\text{lost}} = Q_{\text{heater}}$, where Q_{heater} is equal to the voltage (V) by the current intensity (I)—measured simultaneously—and multiplied by the time the resistance remained lit per hour (Eq. 6). The power provided by the resistance is equivalent to the energy flowing through the shading system.

$$Q_{\text{heater}} = V * I * t \quad 6$$

where V, voltage [V]; I, current intensity [A]; and t, time [s].

Hot box calibration

First, the heat transfer coefficient of the blind box ($U_{\text{exp-blind box}}$) was determined (Eq. 5). In order to achieve this measurement, a mask wall of expanded polystyrene (7.5 cm of thickness) was used to fill in the opening (front face) of the calorimeter box, where later shading systems and glass will be placed. The

U-value of the closed box—$U_{\text{exp-blind box}}$—is 1.04 ± 0.13 W/m^2 K. This value includes flanking heat loss and wall heat loss of the hot box.

Measurement and calculation of U-value of shading device

With this same method, but replacing the mask wall from the front face of the box by the shading system under analysis, the energy flow is measured: $U_{\text{exp-shading}}$. From these two values—$U_{\text{exp-shading}}$ and $U_{\text{exp-blind box}}$—the overall heat transfer coefficient of the shading system under study is calculated, according to Eq. 7:

$$U_{\text{shading}} = U_{\text{exp}-\text{shading}} - U_{\text{exp}-\text{blind } box} \quad (7)$$

Figure 5 shows an example of the 16 temperature curves during the temperature stabilization inside the hot box. After three and a half hours, the box reaches steady state. The final value of SHGC and U-factor was obtained as an average from measurements performed 4 times for each of the shading systems studied. This allows the calculation of the error of the measurement.

Fig. 5

Line graph showing inside temperature curves

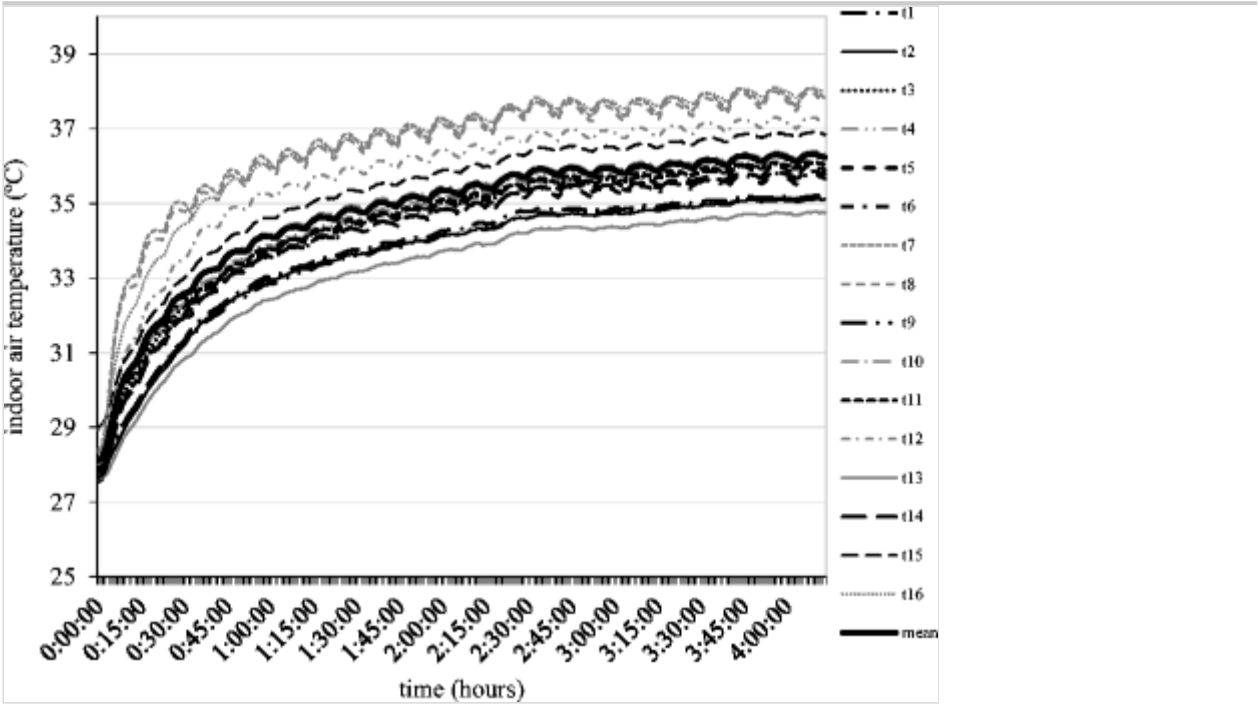

Measurement and calculation of SHGC

For the SHGC measurement, the lamp (solar simulator) is placed in front of the box. Heat gains through the shading system are balanced by energy extracted through the heat exchanger. Once steady state is reached, the temperature of the

inlet and outlet cooling fluid is measured. As this flow is maintained constant ($\dot{m}$ = 0.0769 kg/s), the energy gained by the system is calculated (Eq. 9).

In steady state, the energy flow through the shading system (Q) (Eq. 11) was calculated as the sum of the amount of heat removed by the absorber plate (Q_s) (Eq. 9) and heat exchanged (Q_t) (Eq. 10) per difference of temperature between the interior and exterior of the box. Thus, the energy balance is as follows (Eq. 8):

$$Q\,[\mathrm{W}] = Q_s\,[\mathrm{W}] + Q_t\,[\mathrm{W}] \tag{8}$$

AQ4

Where:

$$\dot{Q}_s\,[\mathrm{W}] = \dot{m}\left[\frac{\mathrm{kg}}{\mathrm{s}}\right] * \mathrm{Cp}\left[\frac{\mathrm{J}}{\mathrm{kg} * \mathrm{K}}\right] * (T_{f,o}\,[\mathrm{K}] - T_{f,i}\,[\mathrm{K}]) \tag{9}$$

$$\dot{Q}_t\,[\mathrm{W}] = U_{exp}\left[\frac{\mathrm{W}}{\mathrm{m}^2 * \mathrm{K}}\right] * A\left[\mathrm{m}^2\right] * (T_i\,[\mathrm{K}] - T_o\,[\mathrm{K}]) \tag{10}$$

$$\begin{aligned}\dot{Q}\,[\mathrm{W}] = {} & \dot{m}\left[\tfrac{\mathrm{kg}}{\mathrm{s}}\right] * \mathrm{Cp}\left[\tfrac{\mathrm{J}}{\mathrm{kg\,K}}\right] * (T_{f,o}\,[\mathrm{K}] - T_{f,i}\,[\mathrm{K}]) + \\ & U_{shading}\left[\tfrac{\mathrm{W}}{\mathrm{m}^2 * \mathrm{K}}\right] * A_{shading}\left[\mathrm{m}^2\right] * (T_i\,[\mathrm{K}] - T_o\,[\mathrm{K}]) + \\ & U_{exp\text{-}blind\ box}\left[\tfrac{\mathrm{W}}{\mathrm{m}^2 * \mathrm{K}}\right] * A_{box}\left[\mathrm{m}^2\right] * (T_i\,[\mathrm{K}] - T_o\,[\mathrm{K}])\end{aligned} \tag{11}$$

where $\dot{m}$, cooling fluid flow rate, [kg/s]; Cp, cooling fluid-specific heat [J/kg K]; $A_{shading}$, area of the shading device [m^2]; A_{box}, area of 5 walls of the box [m^2]; $T_{f,o}$, temperature of the outlet cooling fluid [K]; $T_{f,i}$, temperature of the inlet cooling fluid [K]; T_i, indoor temperature in steady state [K]; T_o, outdoor temperature in steady state [K]; U

AQ5

$_{shading}$ [W/m^2 K]; and $U_{exp\text{-}blind\ box}$ [W/m^2 K].

Based on the foregoing, the $SHGC_{shading}$ is defined as the ratio between the energy flow through the shading system (Q) and the energy striking on the shading system tested (Q_{rad})—as quantified in section 4 (Eq. 12):

$$SHGC_{shading} = Q\,[\mathrm{W}]\,/Q_{rad}\,[\mathrm{W}] \tag{12}$$

Table 3 shows environmental conditions under which measurements of *U*-value and SHGC were performed.

Table 3

Experimental environmental conditions

***U*-value**				**SHGC**		
T_{inside} (°C)	$T_{outside}$ (°C)	h_i (W/m^2 K)	h_o (W/m^2 K)	T_{inside} (°C)	h_i (W/m^2 K)	Direct solar radiation (W/m^2)
35 ± 2%	26 ± 3%	7.5 ± 5%	8 ± 4%	52 ± 2%	9.5 ± 5%	703 ± 10%

Results

U-value measurements

Table 4 shows *U*-values for each of the shading systems studied: clear glass (3 mm); interior drapery curtain: organza, jacquard, polyester gabardine; horizontal interior venetian blind (slat width 17 mm; tilt angle 0° and 45°): diffuse silver, diffuse white; and solar control film: fxst20, fxst35, and p18ar.

Table 4

U-values: clear glass (3 mm); interior drapery curtain: organza, jacquard, polyester gabardine; solar control film: fxst20, fxst35, and p18ar; horizontal interior venetian blind (slat width 17 mm; tilt angle 0° and 45°): diffuse silver, diffuse white

Shading device	Measured *U*-value (W/m^2 K)	Standard deviation	Uncertainty (%)
Clear glass 3 mm	3.86	0.43	11.07
Polyester gabardine	3.37	0.52	15.45
Organza	3.58	0.50	13.97
Jacquard	3.33	0.42	12.48
fxst20	3.81	0.48	12.60
p18ar	3.84	0.53	13.68
fxst35	3.82	0.53	13.87
Diffuse white venetian blind (0°)	3.21	0.41	12.77
Diffuse white venetian blind (−45°)	3.04	0.42	13.67

Shading device	Measured *U*-value (W/m K)	Standard deviation	Uncertainty (%)
Diffuse silver venetian blind (0°)	3.15	0.45	14.29
Diffuse silver venetian blind (−45°)	3.05	0.45	14.75

It is observed, as assumed a priori, that the highest *U*-value is that of clear glass (3 mm) ($U = 3.86 \pm 0.43$ W/m^2 K) (Table 4).

Regarding the analyzed textiles, it was detected that both textiles which have the lowest opening factor and increased thickness (gabardine and jacquard) show *U*-values of 3.37 ± 0.52 and 3.33 ± 0.42 W/m^2 K, respectively (Table 4), whereas organza textile, which displays an increased openness factor and lower thickness, has a *U*-value of 3.58 ± 0.50 W/m^2 K. Based on this information, we conclude that gabardine and jacquard have the highest thermal insulation capacity of the fabric materials studied. The heat transfer through gabardine and jacquard is less than that of organza, which is the less insulating textile.

Regarding solar control filters, we can observe broadly that they do not improve glass insulation significantly. *U*-values obtained for the solar control filters are as follows: fxst20, 3.81 ± 0.48 W/m^2 K; fxst 35, 3.82 ± 0.53 W/m^2 K; and 3.84 ± 0.53 W/m^2 K for silver filter (p18ar) (Table 4). This thermal behavior is similar to that of glass since films have a thickness of 50 μm and thermal conductivity (k) close to 1 W/m K.

Scenarios with venetian blinds exhibit lower *U*-values (white venetian blind (0°), 3.21 ± 0.41 W/m^2 K; white venetian blind (−45°), 3.04 ± 0.42 W/m^2 K; silver venetian blind (0°), 3.15 ± 0.45 W/m^2 K; silver venetian blind (−45°), 3.05 ± 0.45 W/m^2 K) when compared to single glazing and solar control films. Venetian blinds have closer *U*-values to those of the thickest textiles (Table 10). It is observed that the heat transfer coefficient is sensitive to variations in slat angle. This may be due to the physical properties of the system itself or to the uncertainty of the measurement method used.

AQ6

The overall *U*-value of the closed box ($U_{\text{exp-blind box}} = 1.04 \pm 0.13$ W/m^2 K), insulated with 7.5 cm polystyrene, is lower than that of the other analyzed conditions. As the closed box is well-insulated, the effects of h_i and h_o are negligible. Whereas in the conditions where shading devices are tested, slight changes in the thermal resistance of internal-external air layers strongly affect

the *U*-value of the system; this is why *U*-values show a higher standard deviation.

SGHC, solar heat gain coefficient

Table 5 shows SGHC values measured in a calorimeter for shading systems examined in this paper.

Table 5

SHGC values: clear glass (3 mm); interior drapery curtain: organza, jacquard, polyester gabardine; solar control film: fxst20, fxst35, and p18ar; horizontal interior venetian blind (slat width 17 mm; tilt angle 0° and 45°): diffuse silver, diffuse white

Shading device	SHGC measured	Standard deviation	Uncertainty (%)
Clear glass 3 mm	0.87	0.04	4.77
Polyester gabardine	0.73	0.03	4.81
Organza	0.82	0.04	4.88
Jacquard	0.69	0.04	6.14
fxst20	0.66	0.04	5.55
p18ar	0.34	0.02	4.54
fxst35	0.67	0.04	5.27
Diffuse white venetian blind (0°)	0.73	0.04	5.47
Diffuse white venetian blind (−45°)	0.48	0.02	4.3
Diffuse silver venetian blind (0°)	0.77	0.02	3.67
Diffuse silver venetian blind (−45°)	0.49	0.02	3.14

Regarding the values of SHGC, it can be seen that the single-pane glass shows the highest SHGC, 0.87 ± 0.04 (Table 5). This is because this scenario has the highest solar transmittance (0.834), since no shading element is interposed.

Interior textile curtains show reduced values of SHGC when compared with single-pane glass (Table 5). The organza fabric presents the highest SHGC (0.82 ± 0.04). This is because this textile has a higher openness factor and thinner spinning. The jacquard textile has the lowest solar radiation transmittance (SHGC 0.69 ± 0.04) of the three fabrics studied. While this textile

features an openness factor similar to gabardine, it is thicker (0.9 mm). The SHGC of gabardine is intermediate with respect to the other two textiles (0.73 ± 0.03). It is noted that for this type of shading system, the higher the SHGC, the higher the *U*-value.

Applied film p18ar is the shading system with the lowest SHGC (0.34 ± 0.02) (Table 5). This is due to the high reflectance of the system that prevents the entry of radiation in the near-infrared range of the solar spectrum (800–2500 nm) (Fig. 6). The transmittance in the near-infrared spectral range is augmented through fxst20 and fxst35 filters (Figs. 7 and 8), wherein the SHGC is 0.66 ± 0.04 and 0.67 ± 0.04, respectively. Even though they showed transmittances in the order of 20 and 35% for wavelengths ranging from 350 to 750 nm (visible solar radiation), transmittance increases in the near-infrared range. Spectral selectivity data is provided by OPTICS6.0 (LBNL 2013).

Fig. 6

Line graph showing spectral transmittance and reflectance of p18ar filter (Optics6, LBNL, International Glazing Data Base)

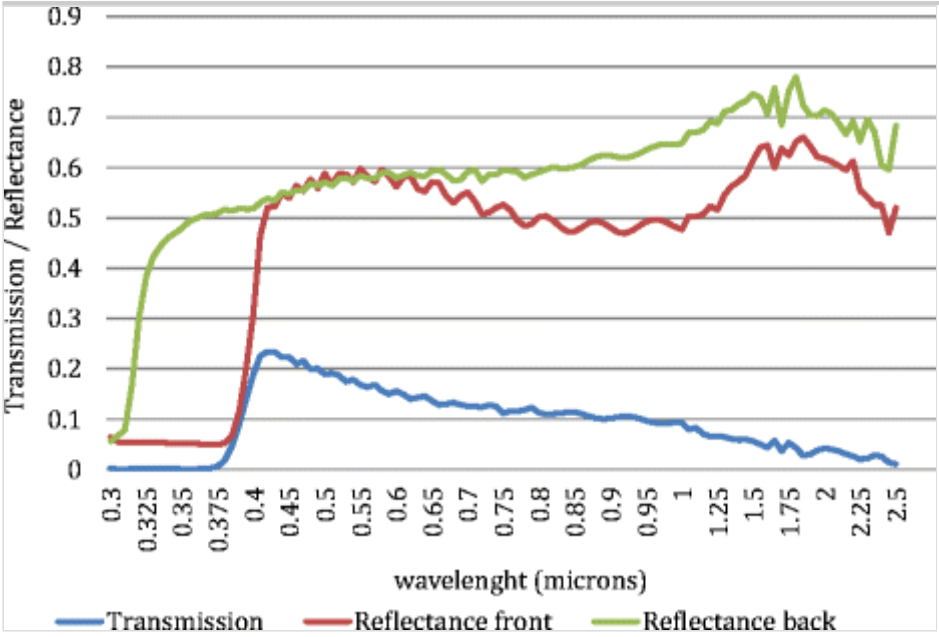

Fig. 7

Line graph showing spectral transmittance and reflectance of fxst20 filter (Optics6, LBNL, International Glazing Data Base)

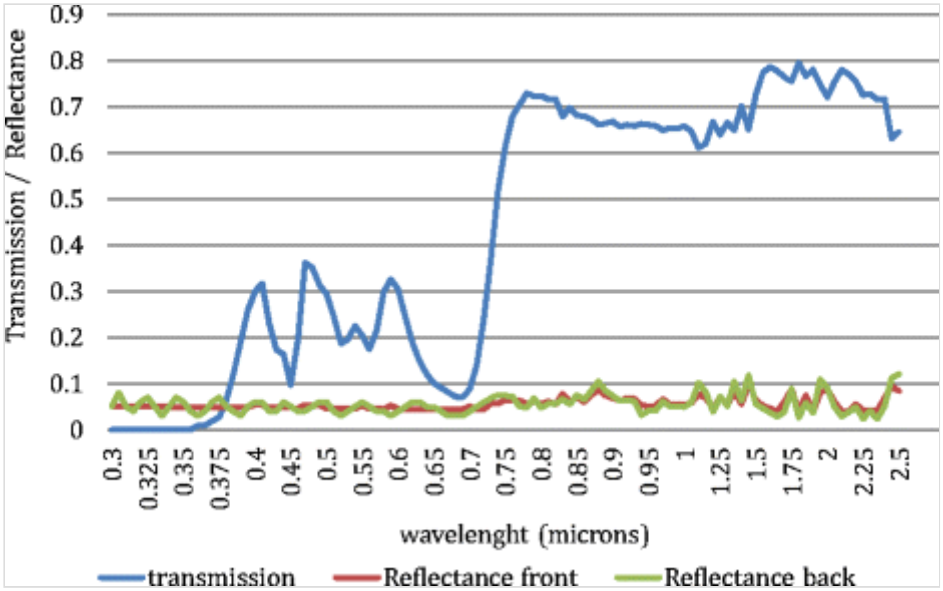

Fig. 8

Line graph showing spectral transmittance and reflectance of fxst35 filter (Optics6, LBNL, International Glazing Data Base)

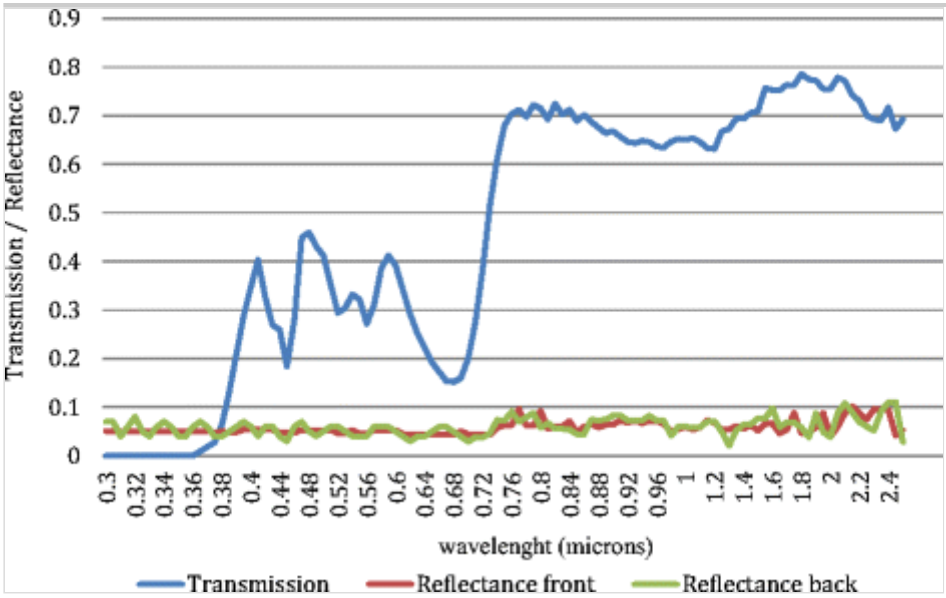

The energy performance of the studied systems concerning the *U*-value is dependent on the thickness and thermal conductivity of the material. Regarding the SHGC, transmittance and absorptance define the behavior of the systems and differ significantly according to the type of shading device analyzed.

For venetian blinds, SHGC is clearly determined by the percentage of opening in accordance with the slat tilt angle (Table 5). The average SHGC is 0.75 for 0° inclination and 0.485 for 45° inclination. Slat position is crucial because it sets the solar permeability, in other words, transmittance. Regarding changes in solar gains caused by the surface properties of the venetian blinds under study, it is

observed that diffuse metallic finish does not significantly change the SHGC of the venetian blind.

Comparisons between measurements and simulation results

U-values and SHGC calculated with Window 6.3 (LBNL 2011) were compared with those obtained through measurement (Tables 6 and 7). For this purpose, boundary conditions in Window 6.3 were set according to the environmental conditions in which measurements were performed (Table 3).

Table 6

Comparison of simulated (Window 6) and measured *U*-value

Shading device	Measured *U*-value (W/m^2 K)	Simulated *U*-value (W/m^2 K)	Standard deviation	Relative error (%)
Clear glass 3 mm	3.86 ± 0.43	3.95	0.06	2.33
Polyester gabardine	3.37 ± 0.52	2.77	0.42	17.80
Organza	3.58 ± 0.50	3.15	0.30	12.01
Jacquard	3.33 ± 0.42	2.77	0.40	16.82
fxst20	3.81 ± 0.48	3.9	0.06	2.36
p18ar	3.84 ± 0.53	3.95	0.08	2.86
fxst35	3.82 ± 0.53	3.91	0.06	2.36
Diffuse white venetian blind (0°)	3.21 ± 0.41	3.26	0.04	1.56
Diffuse white venetian blind (−45°)	3.04 ± 0.42	3.07	0.02	0.99
Diffuse silver venetian blind (0°)	3.15 ± 0.45	3.26	0.08	3.49
Diffuse silver venetian blind (−45°)	3.05 ± 0.45	3.07	0.01	0.66

Table 7

Comparison of simulated (Window 6) and measured SHGC

Shading device	SHGC measured	SHGC simulated	Standard deviation	Relative error (%)
Clear glass 3 mm	0.87 ± 0.04	0.88	0.00	1.15
Polyester gabardine	0.73 ± 0.03	0.16	0.40	78.08

Shading device	SHGC measured	SHGC simulated	Standard deviation	Relative error (%)
Organza	0.82 ± 0.04	0.46	0.25	43.90
Jacquard	0.69 ± 0.04	0.16	0.37	76.81
fxst20	0.66 ± 0.04	0.69	0.02	4.55
p18ar	0.34 ± 0.02	0.3	0.03	11.76
fxst35	0.67 ± 0.04	0.71	0.03	5.97
Diffuse white venetian blind (0°)	0.73 ± 0.04	0.78	0.04	6.85
Diffuse white venetian blind (−45°)	0.48 ± 0.02	0.5	0.01	4.17
Diffuse silver venetian blind (0°)	0.77 ± 0.02	0.78	0.01	1.30
Diffuse silver venetian blind (−45°)	0.49 ± 0.02	0.5	0.01	2.04

Window 6.3 was used to perform the simulations because it has an extensive glazing and shading database and it is updated by its developers (Curcija 2016). Also, this software is used in other Latin American countries for window energy performance certification (Milbratz 2007).

Boundary conditions

It is well known that thermal transmittance of fenestration is dependent on the environmental conditions on the indoor and outdoor sides (Chen and Wittkopf 2012; ASHRAE 2009). This is why the software used to determine the thermal and solar properties of fenestration systems have detailed sections that set boundary conditions. In Window 6.3, boundary conditions are defined by outside air temperature, inside air temperature, inside and outside convection, and inside and outside radiative coefficients or combined heat transfer coefficient and direct solar radiation.

Indoor air temperature (calorimeter box) and outside air temperature (laboratory) (Table 3) were measured as detailed in the “Data acquisition system” section of this work. Incident irradiance (Table 3) was determined as instructed in the “Solar simulator” section.

Combined outside heat transfer coefficient In this work, exterior measurement conditions (inside the laboratory) are consistent with an interior room with natural convection conditions. Because convective and radiative

coefficients are difficult to calculate, various international regulations propose standard values of indoor combined coefficients (radiative-convective), which are used to estimate energy transfer processes in buildings (Table 8).

Table 8

Inside combined coefficient (h_i) [W/m^2 K] (Monroy 1995)

Heat flow direction	España/NBE CT-79, annex 3	Britain. Burberry, p. 51	USA/ASHRAE Fund. 75, p. 357
0° rises	11.11	9.09	9.26
45°	–	–	9.08
90° horizontal	9.09	8.33	8.29
135°	–	–	7.49
180°	5.88	6.67	6.13

From all radiative-convective models that Window 6.3 provides, the combined coefficient model (radiative-convective) was selected for calculation of the heat transfer coefficient. The standard value used in this coefficient is 8 W/m^2 K, calculated according to Eq. 13:

$$h_{\mathrm{i}} = 3.6 + \left(4.4 * \frac{\varepsilon}{0.837}\right) \left[\mathrm{W/m^2\,K}\right] \tag{13}$$

where 3.6 [W/m^2 K] is the convective component of the combined coefficient, (4.4 * ε/0.837) is the radiative component of the combined coefficient, and ε is the emissivity of the glass surface (LBNL 2009).

As measured by Wall and Bülow-Hübe (2003), this value can vary slightly because of the airflow caused by the air conditioning system. According to their measurements, this airflow increases the convective coefficient up to 3.9 W/m^2 K.

Combined inside heat transfer coefficient Combined inside heat transfer coefficient was calculated through Eq. 14, proposed by the ASHRAE (2009), for indoor surface heat transfer coefficient for vertical orientation surface in still air conditions.

$$h_{\mathrm{i}} = h_{\mathrm{ic}} + h_{\mathrm{iR}} = 1.46(\Delta T/L)^{0.25} + \varepsilon\sigma\left(T_{\mathrm{i}}^4 - T_{\mathrm{g}}^4\right)/\Delta T \tag{14}$$

where ΔT, $T_i - T_g$ [K]; L, glazing height [m]; T_g, glass temperature [K]; σ, Stefan-Boltzmann constant; and ε, surface emissivity (ASHRAE 2009).

Glass surface temperature (T_g = 33.2 °C ± 2% (U-value)/T_g = 37.5 °C ± 3% (SHGC)) was measured with two pairs of thermocouples fixed to the glazing. The calculated value is 7.5 W/m^2 K ± 5% for U-value measurement and 9.5 W/m^2 K ± 5% for SHGC measurements. In the test measurement carried out by Kuhn (2014) using the cool box method with a high emissivity sample, he determined a h_i of 8 W/m^2 K.

Combined inside heat transfer coefficient was assessed through this method because of the availability of the information needed for its calculation and also because we are not able to make the calibration transfer standard tests (CTS) carried out to achieve convection coefficients (Kuhn 2014; Chen and Wittkopf 2012; Collin 2004a) in the test facility featured. However, it should be considered that this decision entails a substantial simplification because it does not take into account the impact of the shading device in the final values of inside convective and radiative coefficients (Collins and Wright 2006; Collins 2004a; Ye et al. 1999). In complex fenestration, convective heat transfer between nonadjacent layers can occur (Collins 2004a). Also, shading layers are inherently diathermanous meaning that they transmit both long- and shortwave radiation. Radiative heat transfer can also occur between nonadjacent layers (Collins and Wright 2006; Wright 2008; ASHRAE 2009). Some studies show that convective coefficients have a greater impact on U-value than on SHGC (Collins 2004b). Moreover, a computer-based simulation study published by Foroushani et al. (2016) states that the presence of an indoor-mounted attachment can significantly change the solar heat gain coefficient of a fenestration system. Nevertheless, the solar heat gain coefficient and the overall heat transfer coefficient are not sensitive to the indoor convection coefficient (Foroushani et al. 2016).

This issue is also present in many softwares (Window 6 (LBNL 2008); Para-Sol (Wall and Bülow-Hübe 2003) used to calculate U and SHGC, as a limitation of indoor shading device calculation models. Current fenestration thermal models (ISO 15099 2003), which are implemented in existing fenestration design tools such as WINDOW and WIS, do not account for such effects of complex fenestration systems (Laouadi 2009). Recent research showed that these simple models were not accurate for slat-type blinds (Yahoda and Wright 2004; Laouadi 2009) and for diathermanous (infrared transparent) layers (Collins and Wright 2006; Laouadi 2009). When shading devices are analyzed, radiative and

convective heat transfer from the inner glass may or may not occur with the shade. This makes the thermal resistance network much more complex. In both cases, the system becomes significantly more difficult to analyze when a shade is added. Existing procedures of analysis are based on the assumption that all layers in the window are opaque to longwave radiation, and this is not correct for diathermanous shading layers (Collins and Wright 2006).

Measurements and simulation results

Concerning *U*-values (Table 6) of single glass (3 mm), applied films, and horizontal inside venetian blinds, there is an acceptable level of agreement between simulated and measured values (difference under 2.86%). Whereas inside textile curtain, *U*-values show differences between 12.01 and 17.8%.

Regarding the SHGC (Table 7), we detect that glass, applied films, and horizontal venetian blinds show SHGC disagreements under 11.76%. Textiles exhibit discrepancies exceeding 78%. Organza (thinner textile with greater openness factor) has the lowest average difference (43.9%). This could be caused by the WOVENSHADE model not presenting an adequate level of adjustment for SHGC calculation.

Analysis and discussion of results

With regard to blinds, as observed in other studies (Shahid and Naylor 2005; Sharda and Kumar 2014; Dubois 1997), *U*-value results show that the presence of a venetian blind improves the energy performance of single-glazed windows. Shahid and Naylor (2005) concluded that one of the reasons *U*-value decreases is that the presence of blinds reduces the radiative heat. Furthermore, the results of the current study show that venetian blinds reduce the *U*-value of the single glazing by 17% when slats are fully opened (0°) and by 21% when slats angle is increased (45°). Shahid and Naylor (2005) determined that the blind reduces the *U*-value of a single-glazed window by 11% when it is fully opened and by 15% at 45°. Because the analyzed venetian blinds do not have the same geometrical and optical properties, differences between both studies in terms of the *U*-value regarding slat angles are detected (Collins et al. 2002). According to the work carried out by Shahid and Naylor, the *U*-value increases more significantly when slats are set between 30° and 60° for a single-glazed window. They explain that this behavior is caused by the “chimney effect,” which enhances the convective heat transfer at the indoor glazing. Future studies must be done with increased angle louver adjustments (>45°) in order to identify changes in the *U*-value for the analyzed blinds. Regarding SHGC, interior horizontal venetian blinds modify their solar gain according to the slat angle. The closer to the horizontal position the slats are arranged, the higher the solar heat gain. In this study, an

average decrease of 15% for fully opened blind and of 45% for 45° louver inclination with respect to single glazing is found. This is because the slat inclination determines the percentage of openness of the system and therefore its solar transmittance. SHGC ratio (SHGC shading device/SHGC single pane) according to louver angle for both white and metallic surface was estimated; results achieved in these work were compared to the results obtained by Wall and Bülow-Hübe (2003). It was found that differences in solar gain due to slat angle in both studies are similar; white blinds show the highest difference (under 12%). This difference is possibly explained by the fact that we are comparing a double-pane window with a single-pane window and because optical and geometrical properties of the blinds are not identical.

Regarding interior textile curtains, *U*-values found are between 3.33 and 3.81 W/m^2 K. Jacquard and gabardine curtains showed an average reduction of 13% compared to single glazing, while the organza curtain reduces the *U*-value only by 7%. According to *Architect's Journal* (Dubois 1997), the effectiveness of curtaining for insulation is largely a product of the layer of still air trapped between the curtain and the glass. Organza fabric has a high openness factor (0.45) and, therefore, has inferior insulation properties. A study carried out by the Department of Energy in 1990 (Dubois 1997) shows that lined curtains have a significant effect on window heat loss achieving a 20% reduction. It is observed that for interior textile curtains, SHGC rises with increasing openness factor (polyester gabardine: openness factor 0.05, SHGC 0.73; jacquard: openness factor 0.05, SHGC 0.69; organza: openness factor 0.45, SHGC 0.82). In addition, it can be seen that the higher the solar factor, the greater the heat transfer coefficient. It is difficult to compare obtained results with those achieved in other studies because of the absence of clear criteria that determines material properties and because most of the tests are done with double-pane arrangements. However, the shading coefficient (0.5) determined by the Department of Energy in 1990 for permanently closed curtains for single-pane windows is a useful reference value (Dubois 1997). Regarding the performance of curtains with double-pane windows, Wall and Bülow-Hübe (2003) measure values of 0.45 for off-white pleated curtains and Kotey et al. (2009) 0.43 for beige closed weave plated drapes. Considering the widespread use of such shading systems, more research must be done concerning fabric curtains because few studies characterize their energy performance. However, in order to produce comparable data, it is necessary to set clear and objective description criteria.

In general, we can say that the shading devices studied show an average SHGC of 0.67, comparable to the average SHGC (0.6) measured by Wall and Bülow-Hübe (2003) for indoor shading device (venetian blinds, pleated curtains, roller blinds, screen fabric, and solar control films).

Regarding simulation results, it can be further observed that *U*-values calculated through simulation in Window 6.3 show an average difference of 5.75%. Despite limitations of heat transfer phenomena models between glazing and indoor shading device, the compared measured and simulated values show acceptable agreements considering that the highest difference found is 17.8% (indoor drapery curtain). Concerning venetian blinds, the low slat angles studied (0 and 45) may be one of the reasons why the *U*-value differences are under 3.49%. Shahid and Naylor (2005) state that the presence of blinds has a strong effect on the convective heat transfer from the indoor glazing except when the blind is close to fully open. When blind louvers are fully closed, the convective heat transfer from the indoor glazing increases by 22% (Shahid and Naylor 2005).

SHGC obtained through simulation must be analyzed in two separate groups. The group consisting of solar films and venetian blinds shows differences between simulated values and measured values under 11.76%. Furthermore, these differences increase to 78.08% for indoor drapery curtains. The study, led by Jonsson et al. (2008), compares values of direct hemispherical transmittance as a function of angle of incidence according to the WOVENSHADE model (radiosity) and from a complete bidirectional scattering distribution function (BSDF) generated with TracePro (raytracing). Significant differences were identified in the transmittance and they suggest that the diffuse component calculated by the model is very small, probably zero. Therefore, currently, many textiles employed as shading elements have been characterized by BSDF and are part of the CGDB (complex glazing database) Version 1.2. used by Window 6.3. Nonetheless, these databases are not easy to assemble because measuring equipment is very expensive and because data processing is not easy to achieve. This solidifies the importance of developing models that adequately assess *U*-value and SHGC calculation.

In addition, it is important to note that the Lawrence Berkeley National Laboratory–US Department of Energy currently have a project focused on fenestration attachments 2013–2018 (Curcija 2016). One of the main objectives of this project is to develop validated simulation models and procedures for characterizing properties and energy impacts of a wide range of window attachments. Validated algorithms and databases developed during this project provide the necessary credibility for simulation tools that will be used for rating and certification (Curcija 2016).

Conclusion

This paper presents the use of a low-cost hot-cold box calorimeter as an empirical laboratory method for determining the solar factor and overall heat

transfer coefficient of shaded interior glazing systems. It can be concluded that the low-cost hot-cold box calorimeter adequately characterizes the energy performance—*U*-value and SHGC—of indoor shading systems (venetian blinds, drapery curtains, solar films). This is particularly important considering the local status of technology and the availability of this type of test facilities. It is also relevant as most of the systems used locally do not have *U*-value or SHGC calculated. However, as many authors state (Wall and Bülow-Hübe 2003; Lomanowski 2008), further developments and validations need to be carried out, especially regarding convective heat transfer, which could influence both measurements and calculation results for internal shading devices.

AQ7

By comparing *U*-value and SHGC calculated through measurement and simulation, this paper does not aim to perform a validation of the Window 6 software. Results obtained through measurement in the cool-hot box calorimeter are compared with those calculated through simulation (Window 6.3) in order to examine and deeply discuss the capability of the model for calculating *U*-value and SHGC of local shading devices, as this software is widely used in the energy certification process. *U*-value differences under 17.8% were found for all the studied shading devices. Also, differences under 11.76% in SHGC were seen for solar films and venetian blinds. However, indoor drapery curtains show differences in SHGC of up to 78.08%.

In order to begin the energy certification process of complex fenestration systems, it is necessary to develop and test measuring equipment as analysis of simulation models employed in other countries. In many cases, certifications in Argentina admit the use of software developed in other countries without evaluating their response to the characteristics of the local building components and without knowing their limitations regarding the calculations of the energy certification indices. Furthermore, it is noteworthy that, in countries where the energy labeling of windows is in effect, the main difficulty for implementation has been the shortage of physical testing laboratories, particularly those with calorimeters for transparent surfaces. These types of study, nationally, allow progress toward solar control system energy labeling.

Acknowledgements

AQ8

This work was funded by the project PICTO ENARGAS 2009-0133: Desarrollo y Estudio de Comportamiento Energético de Precisión de Carpinterías Exteriores y Elementos de Control Solar de Bajo Costo; PICT FONCYT-AGENCIA N° 2089; Iluminación natural en el hábitat de clima soleado; FONCYT, Agencia

Nacional de Promoción Científica y Tecnológica, Argentina; and ENARGAS (Ente Nacional Regulador del Gas).

Compliance with ethical standards

Conflict of interest The authors declare that they have no conflict of interest.

Appendix

Description of solar control systems selected

Horizontal interior venetian blind

The most frequently used types of blinds in the study area are the interior horizontal aluminum venetian blinds and 17-mm-wide slats, and these bands rotate on its horizontal axis regulating light passing between them (Dino Conte 2014).

Geometric properties of the slats were determined using measuring instruments. The obtained dimensions are shown in Fig. 9: the radius of curvature *R*, the strap thickness, strap width, and amplitude of the curvature of the strap (Fig. 9). Table 9 shows the optical properties of materials that make up venetian blinds. The distance between the slat center of the venetian blind is 13 mm.

Fig. 9

Geometric properties of venetian blind slat

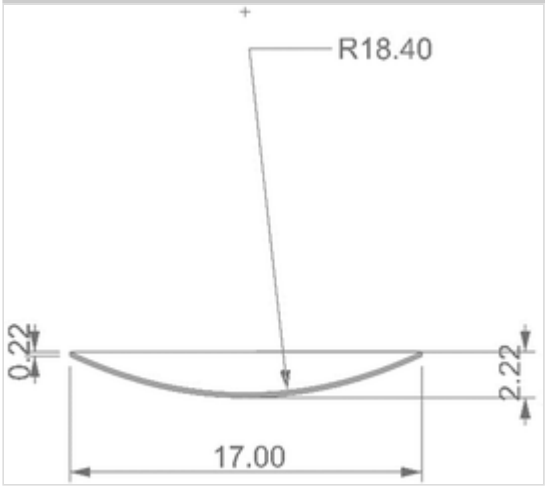

Table 9

Optical properties of surface materials that make up venetian blinds (Huizenga et al. 2013; Laouadi 2011)

	Abs.	Spec. refl	Trans	Diffuse refl.
Diffuse silver	0.28	0	0	0.72

	Abs.	Spec. refl	Trans	Diffuse refl.
Diffuse white	0.3	0	0	0.7

Solar control films

Solar control films selected for this study are as follows:

- p18ar: highly reflective mirror polyester film, 50 μm thick, abrasion resistant (3M Rodin 2014)
- fxst20: medium smoke tinted polyester film, 50 μm thick, abrasion resistant (3M Rodin 2014)
- fxst35: clear smoke tinted polyester film, 50 μm thick, abrasion resistant (3M Rodin 2014)

Interior drapery curtain

The interior textile curtains analyzed in this study are (a) organza (openness factor 0.45), (b) jacquard (openness factor 0.05), and (c) polyester gabardine (openness factor 0.05) (Fig. 10, Table 10). All three selected textiles fall into the category of plain weave (Fig. 11) and belong to the category of light colors (Keyes 1967).

Fig. 10

Samples of analyzing textile: **a** organza, **b** jacquard, **c** polyester gabardine

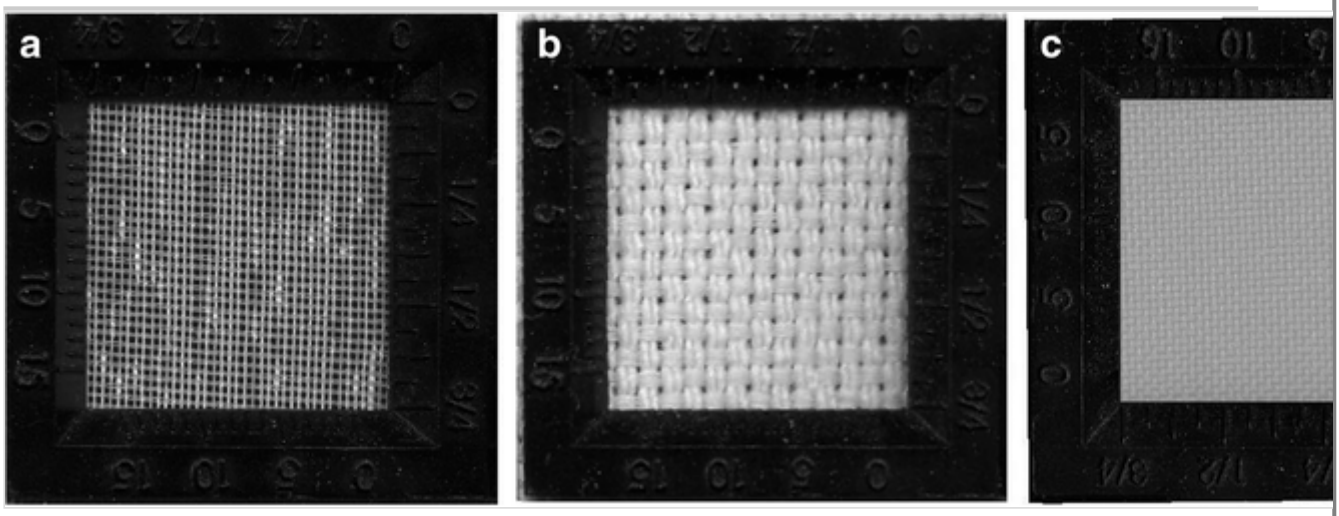

Table 10

Properties of the selected textiles (Textil Network Argentina 2015)

AQ9

	Organza	Polyester gabardine	Jacquard
Density	Low (28 × 28)	26 × 23	High
Weight	30–40 g/m^2	100–150 g/m^2	240–560 g/m^2
Fibers	Silk | polyester | nylon	Polyester 100%	Cotton | synthetic and their blends
Characteristics	Very thin fabric, transparent and brilliant. Shimmering reflections	Smooth, strong, and compact fabric	Drawings embossed with complex design patterns
Main uses	Decorations, sheer curtains. Tablecloth covers	Tablecloths, decoration, curtains. Pants and men's suits. Uniforms	Curtains,upholstery, decoration
Thread diameter (mm)	0.2	0.4	0.8
Spacing between threads (mm)	0.4	0.1	0.2
Fabric thickness (mm)	0.3	0.5	0.9

Fig. 11

Plain weave

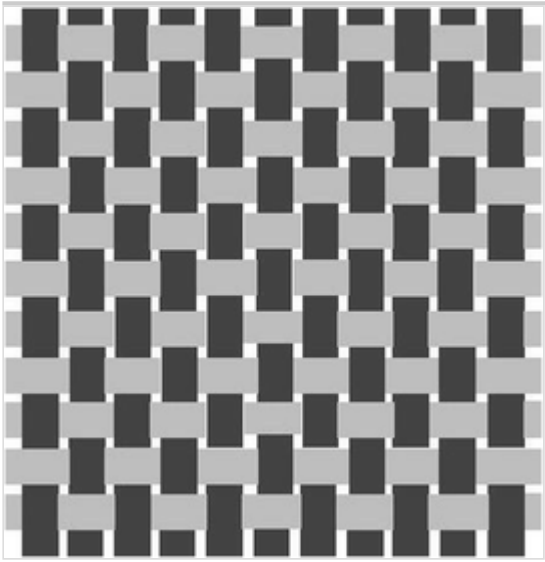

References

Álvarez, G., Palacios, M. J., & Palacios, J. J. (2000). A test method to evaluate the thermal performance of window glazing. *Applied Thermal*

Engineering, 20, 803–812.

ASHRAE. (2009). ASHRAE handbook—fundamentals (SI edition). American Society of Heating, Refrigerating and Air-Conditioning Engineers.

Chaiyapinunt, S., & Khamporn, N. (2014). Heat transmission through a glass window with a curved venetian blind installed. *Solar Energy, 110*, 71–82.

Chaiyapinunt, S., Phueakpongsuriya, B., Mongkornsaksit, K., & Khomporn, N. (2005). Performance rating of glass windows and glass windows with films in aspect of thermal comfort and heat transmission. *Energy and Building, 37*, 725–738.

Chen, F., & Wittkopf, S. K. (2012). Summer condition thermal transmittance measurement of fenestration systems using calorimetric hot box. *Energy and Buildings, 53*, 47–56.

Collins, M. R. (2004a). Convective heat transfer coefficients from an internal window surface and adjacent sunlit venetian blind. *Energy and Buildings, 36*(3), 309–318.

Collins, M.R. (2004b). The importance of indoorand outdoor air-film coefficient measurement to solar calorimetery. SESCI 2004 Conference, University of Waterloo Waterloo, Ontario, Canada, August 21st–25th.

Collins, M. R., & Harrison, S. J. (1999). Calorimetric measurement of the inward-flowing fraction of absorbed solar radiation in venetian blinds. *ASHRAE Transactions, 1999*(105), 1022–1030.

Collins, M. R., & Wright, J. L. (2006). Calculating centre-glass performance indices of windows with a diathermanous layer. *ASHRAE Transactions, 112*, 22–29.

Collins, M. R., Harrison, S. J., Oosthuizen, P. H., & Naylor, D. (2002). Heat transfer from an isothermal vertical surface with adjacent heated horizontal louvers: numerical analysis. *ASME Journal of Heat Transfer, 124*, 1072–1077.

Dino Conte. (2014). Data sheet: veneciana 17mm. Available at: http://www.dinoconte.com.ar/ . Accessed 2 Apr 2015.

Curcija, D. C. (2016). Fenestration attachments. 2016 Building Technologies Office Peer Review. U.S. Energy Department. Lawrence Berkeley National Laboratory (LBNL).

Davidson, M. W. (2017). Tungsten-halogen incandescent lamps. National High Magnetic Field Laboratory, Tallahassee, Florida: The Florida State University. http://zeiss-campus.magnet.fsu.edu/articles/lightsources/tungstenhalogen.html .

Dubois, M. C. (1997). Solar shading and building energy use, a literature review, Part 1. Report TABK--97/3049. Department of Building Science, Lund Institute of Technology, Lund University.

Foroushani, S.S.M., Wright, J.L., Naylor, D. (2016). Sensitivity of the solar heat gain coefficient of complex fenestration systems to the indoor convection coefficient. Hamilton, Ontario, Canada: eSim 2016 Building Performance Simulation Conference, pp. 277–285.

de Gastines, M., Correa, E., & Pattini, A. (2015). Evaluación del balance energético de ventanas en mendoza. Impacto de su tecnología y orientación. *Avances en Energías Renovables y Medio Ambiente, 19*, 05.01–05.12.

Grasso, M. M., Hunn, B. D., & Briones, R. (1990). Effect of textile characteristics on the thermal transmittance of interior shading fabrics. *ASHRAE Transactions, 96*(1), 875–883.

Harrison, S. J., & Collins, M. R. (1999). *Queen's University solar calorimeter —design, calibration, and operating procedure*. Edmonton, Canada: Solar Energy Society of Canada Conference.

Huizenga, C., Arasteh, D., Curcija, C., Klems, J., Kohler, C., Mitchell, R., Yu, T., Zhu, L., Czarnecki, S., Vidanovic, S., & Zelenay, K. (2013). *WINDOW 6.3 shade material library*. Lawrence: Berkeley National Laboratory.

Hutchins, M. (2015). High performance dynamic shading solutions for energy efficiency and comfort in buildings. Sonnergy report 15/498. Sonnergy Limited.

Inoue, T., & Momota, M. (2006). *Simplified on-site method for evaluating solar shading performance of advanced windows*. Geneva, Switzerland: 23rd Conference on Passive and Low Energy Architecture.

International Energy Agency (IEA). (2013). Technology roadmap energy efficient building envelopes. Paris, France. https://www.iea.org/publications/freepublications/publication/TechnologyRoadmap. Accessed 2 Apr 2015.

IRAM 11507. Carpintería de obra. Ventanas y puertas exteriores. Requisitos. parte 6- Etiquetado energético de ventanas.

ISO 15099: 2003. (2003). *Thermal performance of windows. Doors and shading devices*. Berlin: Detailed calculations: BeuthVerlag.

Jonsson, J.C., Lee, E.S., Rubin, M. (2008). Light scattering properties of woven shade-screen material used for daylighting and solar heat-gain control. Optics + Photonics, 7065: 70650R-70650R-11. International Society for Optics and Photonics.

Keyes, M. W. (1967). Analysis and rating of drapery materials used for indoor shading. *ASHRAE Transactions, 73*(1), 8.4.1.

Klems, J. H., & Kelley, G. O. (1996). *Calorimetric measurements of inward-flowing fraction for complex glazing and shading systems*. Atlanta, GA: ASHRAE Winter Meeting.

Klems, J., Selkowitz, S., & Horowitz, S. A. (1982). *Mobile facility for measuring net energy performance of windows and skylights*. Dublin, Ireland: Third International Symposium on Energy Conservation in the Built Environment.

Klems, J. H., Warner, J. L., & Kelley, G. O. (1996). *Calculated and measured SHGC for complex fenestration systems*. Atlanta, GA: ASHRAE Winter Meeting.

Kotey, N. A., Wright, J. L., Barnaby, S. C., & Collins, M. R. (2009). Solar gain through windows with shading devices: simulation versus measurement. *ASHRAE Transactions, 115*, 18–30.

Kuhn, T. E. (2014). Calorimetric determination of the solar heat gain coefficient g with steady-state laboratory measurements. *Energy and Buildings, 84*, 388–402.

Laouadi, A. (2009). Thermal modeling of shading devices of windows. *ASHRAE Transactions, 115*(2), 1–20.

Laouadi, A. (2011). Construction technology updates no. 77: performance of solar shading devices. National Research Council of Canada.

Lau, A. K. K., Salleh, E., Lim, C., & Sulaiman, M. (2016). Potential of shading devices and glazing configurations on cooling energy savings for high-rise office buildings in hot-humid climates: the case of Malaysia. *International Journal of Sustainable Built Environment, 5*, 387–399.

Lawrence Berkeley National Laboratory (LBNL). (2011).THERM 6.3 / WINDOW 6.3 NFRC simulation manual.

Lawrence Berkeley National Laboratory (LBNL). (2009). Calculating fenestration product performance in WINDOW6 and THERM6 according to EN 673 and ISO 10077.

Lawrence Berkeley National Laboratory (LBNL). (2013). OPTICS 6.0. https://windows.lbl.gov/software/optics/optics.html Accessed 17 Jan 2017.

Lawrence Berkeley National Laboratory (LBNL). (2008). WINDOW 6.2 / THERM 6.2. Research Version User Manual. Windows & Daylighting Group, Building Technologies Program, Environmental Energy Technologies Department.

Lomanowski, B.A. (2008). Implementation of window shading models into dynamic whole-building simulation. Thesis. Master of Applied Science in Mechanical Engineering University of Waterloo.

Lunde, H. A., & Lindley, J. A. (1988). Effects of window treatments in cold climates. *Home Economics Research Journal, 16*(3), 223–235.

Marinoski, D. L., Güths, S., & Lamberts, R. (2012). Development of a calorimeter for determination of the solar factor of architectural glass and fenestrations. *Building and Environment, 47*, 232–242.

Milbratz, J. H. (2007). Análise de propriedades térmicas e ópticas de janelas através de simulação computacional. Thesis. Departamento de Engenharia Civil, Centro Tecnológico, Universidade Federal de Santa Catarina.

Monroy, M. M. (1995). Comportamiento térmico de cerramientos soleados. Un modelo de simulación por diferencias finitas. Doctoral Thesis, Departamento de Construcción Arquitectónica, Universidad de Las Palmas de Gran Canaria.

National Program for the Rational and Efficient Energy Use. (PRONUREE) Commercial and public sector, 2015. http://www.energia.gov.ar/contenidos/verpagina.php?idpagina=2901 . Accessed 27 Apr 2015.

Natural Resources Canada. (2017). National Solar Test Facility. Exova Canada Inc., Mississauga (Ontario). http://www.nrcan.gc.ca/energy/renewable-electricity/solar-thermal/7335 . Accessed 17 Jan 2017.

NFRC 200. (2010). *Procedure for determining fenestration product solar heat gain coefficient and visible transmittance at normal incidence*. USA: National Fenestration Rating Council.

Ng, P.K. (2014). Semi-transparent building-integrated photovoltaic (BIPV) windows for the tropics. Doctoral thesis, Department of Architecture, National University of Singapore.

Philips. (2016). Technical sheet (Philips Halogen linear lamp 8727900881264 1000 W R7s cap 220–240 V Warm White). http://www.p4c.philips.com/cgi-bin/cpindex.pl?scy=AR&slg=EN&ctn=8727900881264 Accessed 18 Feb 2017.

3M Rodin. (2014). Data sheet: 1M solar control films.

Selkowitz, S. (2011). The future of building energy efficiency. Progress via global collaboration. Environmental Energy Technologies Division, Lawrence Berkeley National Laboratory.

Shahid, H., & Naylor, D. (2005). Energy performance assessment of a window with a horizontal venetian blind. *Ener. Build., 37*, 836–843.

Sharda, A., & Kumar, S. (2014). Heat transfer through glazing systems with inter-pane shading devices: a review. *Energy Technology & Policy: An Open Access Journal, 1*(1), 23–34.

Sharda, A., & Kumar, S. (2016). Experimental investigation of U value of double-glazed window with inter-pane blinds using Taguchi techniques. *Energy Efficiency, 9*, 1145.

Simmler, H., & Binder, B. (2008). Experimental and numerical determination of the total solar energy transmittance of glazing with venetian blind shading.

Building and Environment, 43, 197–204.

Textil Network Argentina. (2015).Available at: http://www.redtextilargentina.com.ar/ Accessed 2 Apr 2015.

Tzempelikos, A. (2008). A review of optical properties of shading devices. *Advances in Building Energy Research, 2*(1), 211–239.

Wall, M., & Bülow-Hübe, H. (2003). *Report no EBD-R--03/1 Solar protection in buildings. Part 2, 2000–2002. Department of Construction and Architecture*. Lund: Lund University.

Wright, J. L. (2008). Calculating centre-glass performance indices of glazing systems with shading devices. *ASHRAE Transactions1, 14*(2), 199–209.

Yahoda, D. S., & Wright, J. L. (2004). Heat transfer analysis of a between-panes venetian blind using effective long wave radiation properties. *ASHRAE Transactions, 110*(1), 455–462.

Ye, P., Harrison, S. J., Oosthuizen, P. H., & Naylor, D. (1999). Convective heat transfer from a window with a venetian blind: detailed modeling. *ASHRAE Transactions, 105*, 1031–1037.

---

[1] For complex glazing systems, N_i must be determined calorimetrically for a given system geometry and set of emittances but will be the same for all such systems regardless of the solar-optical properties of the layers. Therefore, it only needs to be determined once for a “thermally prototypic” system and can be combined with quantities of transmittance and absorptance determined by noncalorimetric optical techniques to produce values of SHGC for a variety of similar systems (Klems et al. 1996). In another study, Klems presents the results of an extensive set of calorimetric measurements of layer-specific inward-flowing fractions for common thermally prototypic systems involving shading (Klems and Kelley 1996). Collins and Harrison (1999) found that for venetian blinds the inward-flowing fraction is dependent on the interior/exterior temperature difference and only slightly dependent on the absorbed irradiance and exterior air film coefficient. They also checked that blind slat angle has an effect on the inward-flowing fraction under certain circumstances.